FISEVIER

Contents lists available at ScienceDirect

Journal of Colloid and Interface Science

journal homepage: www.elsevier.com/locate/jcis



Regular Article

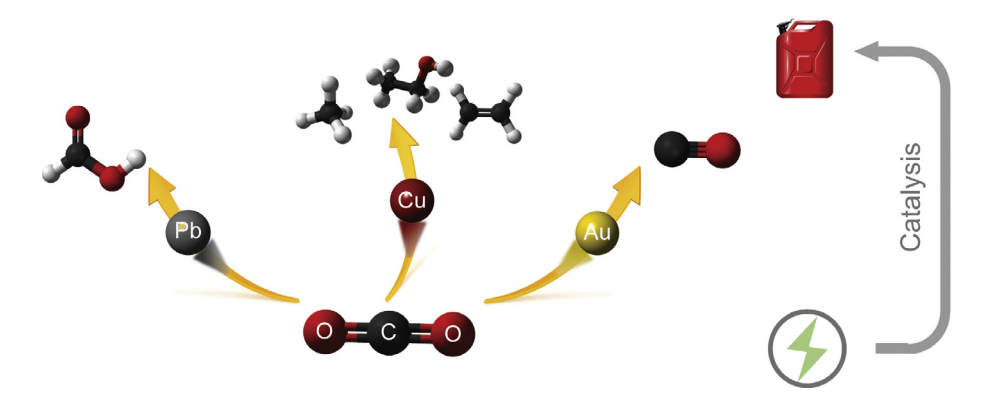
Metallic nanocatalysts for electrochemical CO₂ reduction in aqueous solutions



Yuanxing Wang a,*, Cailing Niu a, Dunwei Wang b,*

- ^a Institute of Advanced Synthesis, School of Chemistry and Molecular Engineering, Jiangsu National Synergetic Innovation Center for Advanced Materials, Nanjing Tech University, Nanjing, Jiangsu 211816, PR China
- ^b Department of Chemistry, Boston College, Merkert Chemistry Center, Chestnut Hill, MA 02467, USA

G R A P H I C A L A B S T R A C T



ARTICLE INFO

Article history: Received 16 March 2018 Revised 11 May 2018 Accepted 15 May 2018 Available online 16 May 2018

Keywords: CO₂ reduction Electrochemistry Nanocatalysts Metal

ABSTRACT

How to effectively and efficiently reduce carbon dioxide (CO_2) to value-added chemicals represent a frontier in catalysis research. Due to the high activation energy needs and the endothermic nature of CO_2 reduction, the reactions are difficult to carry out. When H_2O is present, hydrogen evolution reactions (HER) often compete favorably with CO_2 reduction reactions. For these reactions, catalysts are of critical importance to CO_2 reduction. In this article, we review the various metal nanocatalysts for electrochemical CO_2 reduction (ECR) reactions. In recognition of the importance of H_2O to CO_2 reduction, we focus our discussions on systems in aqueous solutions. Nanostructured metal catalysts are chosen for the discussions because they represent the most effective catalysts for ECR. After a brief introduction of the fundamental principles of ECR, we devote the rest of the article on the discussions of various types of nanostructured metallic catalysts, which are categorized by their compositions and working mechanisms. Lastly, strategies for improving reaction efficiency and selectivity are discussed.

© 2018 Elsevier Inc. All rights reserved.

1. Introduction

1.1. Background of the electrochemical CO₂ reduction

Carbon dioxide $({\rm CO_2})$ is the most stable end products of fossil fuel combustion. Its rapid increase over the past 150 years has

E-mail addresses: ias_yxwang@njtech.edu.cn (Y. Wang), dunwei.wang@bc.edu (D. Wang).

^{*} Corresponding authors.

been regarded as an indication of excessive energy consumption by human activities. The high concentration of CO₂ in our atmosphere is widely agreed as man-made and is a source of recent climate changes [1]. As a way to mitigate the negative impacts by the high concentration of this molecule, the research society has been working hard to convert CO₂ into useful chemicals, particularly liquid fuels [2,3]. On a fundamental level, direct chemical utilization of CO₂ is also interesting because CO₂ represents a low-cost source of C for chemical synthesis. But this conversion is extremely difficult to control due to the rich oxidation states of C in various products, as well as the high activation energies between these products [4–7]. Of the approaches that have been studied, electrochemical CO₂ reduction (ECR) to fuels and value-added chemicals in aqueous solutions is especially appealing since it offers a versatile route toward a wide range of chemicals that can readily meet the thermodynamic energy needs by electricity, which could in principle be supplied by renewable sources such as solar or wind [8].

Exciting progresses notwithstanding, critical issues remain for ECR to become a practicable approach. The main challenges for ECR in aqueous solutions include the high overpotentials, poor catalyst stability, low product selectivity and low faradaic efficiencies (FE) [9]. Moreover, and often more critically, the competing reactions of hydrogen evolution (HER) tend to be kinetically favored due to the relative simplicity of the reactions in comparison with ECR [10]. For these reasons, the goal of selective CO_2 reduction in H₂O at high efficiencies with low hydrogen evolution and good control over the products has attracted tremendous research efforts. Previous research in this area has mainly focused on metal catalysts that are bulk in sizes and morphologies [11]. Recently, nanoscale metal catalysts have emerged as new material platforms for this important reaction due to their unique properties [8,12]. Our purpose of composing this Article is to review research activities in this area, with a focus on nanoscale metal catalysts. We aim to summarize research efforts for new insights into how to move forward in this important research area. The article is organized as follows. We first discuss the basic principles of electrochemical CO₂ reduction reactions and then various types of nanostructured metallic catalysts based on primary products and reaction selectivity are discussed. In addition, common strategies for improving reaction efficiency and selectivity are summarized.

1.2. Basics of electrochemical CO₂ reduction

For the ease of discussions and to provide a basis for our readers, we first define the commonly used terminologies in the literature.

1.2.1. Onset potential

The onset potential is defined as the applied voltage, at which appreciable current densities can be measured. It is important to note that the measured current densities are thought to produce desired products (such as CO or hydrocarbons). During the reaction, the standard reduction potential is often more positive than the onset potential since the electrochemical CO₂ reduction must overcome a kinetic barrier [13]. Within this context, overpotential is defined as the difference between the standard reduction potential and the onset potential. At what current density should the onset potential be measured, however, is an important point of contentions. In principle, the current density should be determined by measuring the intrinsic exchange current densities; in practice, the exchange current density measurements can be cumbersome. Often, the chosen current density is not based on a meaningful theoretical basis but serves as a reference point for easy comparisons of experimental results by different groups under similar conditions.

1.2.2. Fradaic efficiency

The Fradaic efficiency (FE) refers to the percentage of charges (*i.e.* electrons as we are mostly concerned with reduction reactions) used to produce desired products over the overall charges measured. The FE represents the selectivity of the desired products in a reaction, and the FE can be calculated using Eq. (1).

$$\epsilon_{FE} = \frac{\alpha n F}{O} \tag{1}$$

where α is the number of transferred electros, n is the number of mole of a desired product, F represents Faraday's constant (96,485 C mol⁻¹), and Q referrers to the total charge passed [14].

1.2.3. Tafel slope

The Tafel plot referrers to a plot of overpotential versus the logarithm of the current density. The basis for Tafel analysis is the exponential dependence of the current densities on the applied potentials as described by the Butler-Volmer relationship. The analysis is useful for investigating the mechanisms of the reaction and for evaluating the performance of catalysts. For example, a Tafel slope of $\sim\!118~\text{mV}~\text{dec}^{-1}$ is often used to suggest that the formation of the CO_2^- intermediate by the initial one-electron transfer step is the rate-determining step, while a slope of $\sim\!59~\text{mV}~\text{dec}^{-1}$ implies a fast one-electron pre-equilibrium and then a slower chemical reaction as the rate-determining step in the case of ECR [13].

1.2.4. Electrochemical cells

A variety of experimental configurations have been used in the literature for ECR research. For the ease of discussions, we choose one representative lab-scale H-type cell here. The common H-type electrochemical cell in the ECR consists of two compartments, three electrodes, and gas in/out valves. The two chambers are separated by an ion-exchange (commonly proton-exchange) membrane to prevent products cross-over, which would otherwise compromise the desired reactions. Parameters such as ${\rm CO_2}$ pressure, reaction temperatures, pH, and the details of the electrolyte chemical composition are all important in defining the electrochemical behaviors of the cell.

1.2.5. Reaction pathways

 ${\rm CO}_2$ can be converted into a number of products via different electron transfer pathways. Several common transformations by ECR are summarized in Table 1, where the thermodynamic potentials (E^0) associated with the transformations are listed. From these thermodynamic potentials, we can immediately see why ECR is difficult to control – different transformations often feature thermodynamic potentials that are very close. Another important point to make about Table 1 is that although the reduction reactions can

Table 1 Thermodynamic potentials (E^0) for electrochemical CO₂ reduction reaction [15].

Electrode	Reaction	Number of electron transfer	E ⁰ (V) vs. RHE
Cathode	$CO_2 + 2H^+ + 2e^- \rightarrow CO + H_2O$	2	-0.106
	$CO_2 + 2H^+ + 2e^- \rightarrow HCOOH$	2	-0.250
	$CO_2 + 4H^+ + 4e^- \rightarrow HCOH + H_2O$	4	-0.070
	$CO_2 + 6H^+ + 6e^- \rightarrow CH_3OH + H_2O$	6	0.016
	$CO_2 + 8H^+ + 8e^- \rightarrow CH_4 + 2H_2O$	8	0.169
	$2CO_2 + 12H^+ + 12e^- \rightarrow C_2H_4 + 4H_2O$	12	0.064
	$2CO_2 + 12H^+ + 12e^- \rightarrow C_2H_5OH + 3H_2O$	12	0.084
	$2H^+ + 2e^- \rightarrow H_2$	2	0.000
	$CO_2 + e^- \rightarrow CO_2^-$	1	-1.49
Anode	$2H_2O-4e^-\rightarrow O_2+4H^+$	4	1.230

All potentials are referenced against the reversible hydrogen electrode (RHE).

be diverse, we have limited choices in terms of anode reactions. For large scale reactions, H_2O is our only choice as an electron donor. This is also why natural photosynthesis starts with light reactions that split H_2O .

1.3. Advantages of nanoscale catalysts in electrochemical CO₂ reduction

In comparison to bulk catalysts, nanostructured materials feature distinct advantages [14]. For instance, the much smaller sizes translate to high surface areas, which means nanoscale catalysts are of much more active sites per mass or volume [10]. In addition, advancements in nanomaterial synthesis in recent decades have made it possible to controllably expose preferential facets with high density of active sites for improved activity and selectivity as far as catalysis is concerned [16]. Moreover, nanostructured catalysts often exhibit better tolerance to heteroatom impurities that would be highly detrimental in bulk catalysts [17]. Taken as a whole, nanostructured catalysts present new and exciting opportunities for a wide range of chemical transformations, including CO₂ reduction. Next, we expand on the discussions in connection to ECR.

2. Metallic catalysts for CO₂ reduction

The ECR on bulk metal electrodes was studied for decades, and some of the activities have been discussed by a seminal review by Hori [11]. More recent efforts have been primarily focused on nanostructured metallic catalysts for their enhanced catalytic performance towards the ECR [14]. Based on the primary products and binding energy of various intermediates, metal catalysts may be further classified into several subgroups (Fig. 1) [8,11]. The first group includes examples that preferably promote the formation of CO, such as Au, Ag, and Zn. These metals bind CO₂ intermediate but do not further reduce CO. As a result, they normally produce CO as the primary product. The second group includes catalysts that preferably form formate, such as Sn, Pb and In. Metals in this group bind poorly with the CO₂ intermediate. Instead, they promote the formation of formate or formic acid. Copper (Cu) is the only commonly studied metal in group 3 that not only binds with the CO₂ intermediate, but further reduces CO to produce a variety of hydrocarbon products, including multicarbon ones (C_n) [2,13]. These catalysts are summarized based on their elemental compositions below.

2.1. Gold catalysts

Gold (Au) catalysts has been recognized for their good catalytic performance for CO_2 reduction to carbon monoxide (CO) with good selectivity over HER. The ECR on a number of nanostructured Au, including nanoclusters [18], nanoparticles (NPs) [19–23] and nanowires (NWs) [24] has been investigated experimentally and computationally. As a prototypical example, Zhu et al. demonstrated excellent selective catalytic performance of CO_2 to CO on ultrathin Au NWs in aqueous solutions [24]. The optimal 500 nm Au NWs present a high FE_{CO} of 94% with high current densities at -0.35 V (vs. RHE) (Fig. 2). In an effort to improve the catalytic activity of Au NPs with high grain boundaries densities, Feng et al. showed that specific activity for ECR is linearly correlated with grain boundaries surface density on Au NPs on carbon nanotubes (Fig. 2) [23].

2.2. Silver catalysts

Due to the high cost of Au, large-scale usage of Au catalysts in the ECR poses a significant challenge. As such, a great deal of attention has been attracted to find alternatives to Au. Among those studied, Ag-based catalysts stand out. Excellent ECR performance has been demonstrated on a number of nanostructured Ag electrodes, including NPs [25,26], nanocoral [27], NWs [28], and nanoplates [29]. For example, Kim et al. reported that immobilized Ag NPs on carbon support exhibit high FE with low overpotentials for the ECR to CO [25]. The optimal 5 nm sized Ag NPs on carbon support show a high FE_{CO} of 80% with high current density at -0.75 V (vs. RHE) (Fig. 3). Different from Ag NPs, Liu et al. presented that 5-fold twinned Ag NWs with diameters less than 25 nm feature enhanced current densities and increased FEs. The authors achieved a maximum FE of 99.3% (Fig. 3) [28].

2.3. Tin catalysts

As far as cost is concerned, Sn-based catalysts take it one step further and promise for large-scale utilizations. Efficient ECR performance has been reported on nanostructured Sn catalysts [30–32]. For example, Sheng et al. reported selective ECR to formate by using SnO₂ NPs as electrocatalysts [31]. In aqueous solutions, a high FE for formate of 93% at -1.8 V (vs. saturated calomel electrode (SCE)) with high current density was achieved on 5 nm sized Sn catalysts (Fig. 4). The importance of SnO₂ to the efficiency of ECR on Sn was investigated by Chen et al. The results indicate that metal/metal oxide composited materials are indeed promising catalysts for ECR (Fig. 4) [30].

Fig. 1. Reaction mechanisms of ECR on metal catalysts surfaces in aqueous solutions.

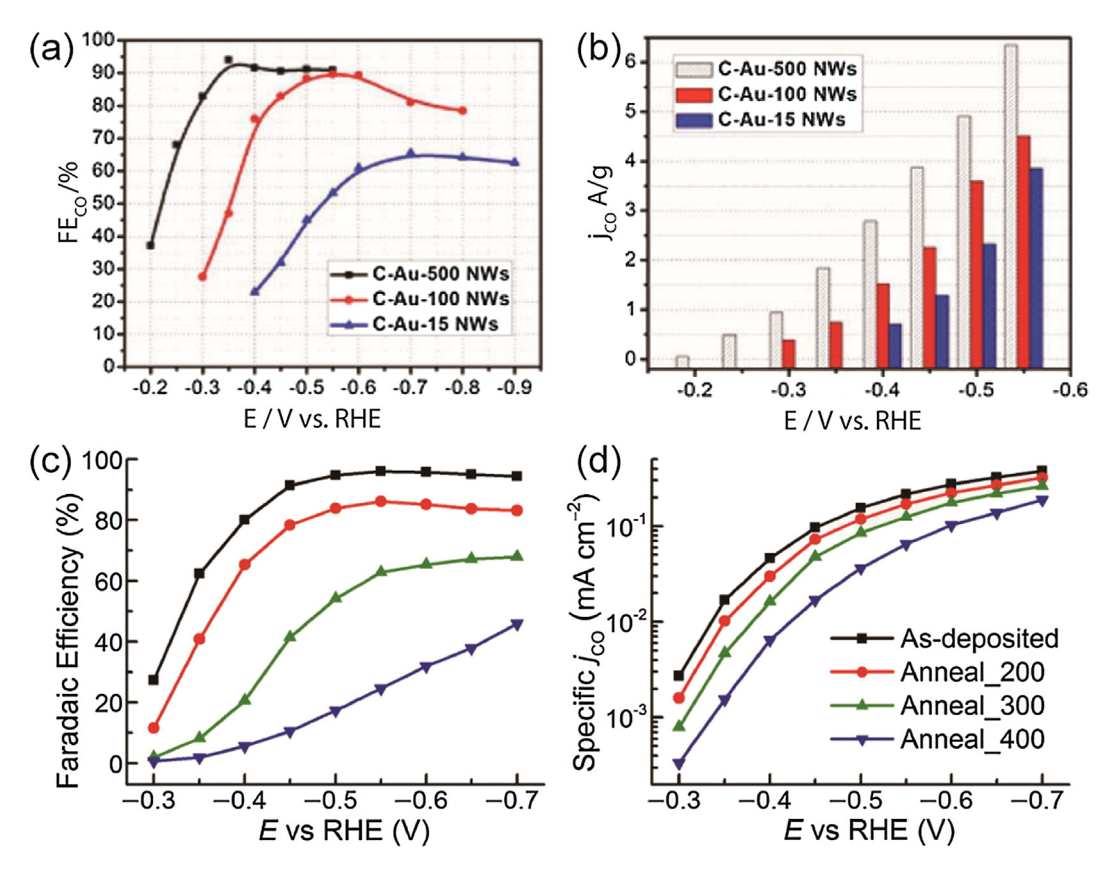


Fig. 2. (a) Potential-dependent FEs of Au NWs on ECR to CO. (b) Potential-dependent current densities (mass activities) on Au NWs. Reproduced with permission from Ref. [24]. Copyright 2014, American Chemical Society. (c) Potential-dependent FEs for CO production. (d) Potential-dependent specific current density for CO production. Reproduced with permission from Ref. [23]. Copyright 2015, American Chemical Society.

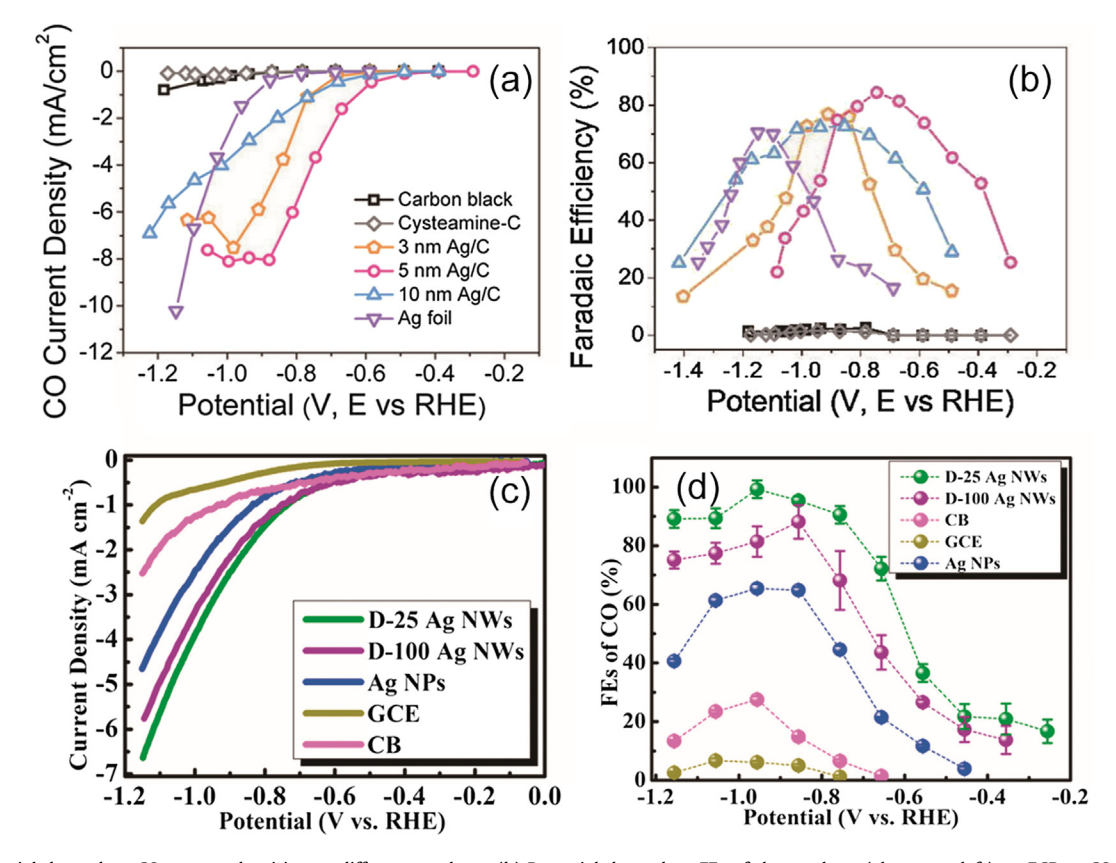


Fig. 3. (a) Potential-dependent CO current densities on different catalysts. (b) Potential-dependent FEs of the catalysts (shown on left) on ECR to CO. Reproduced with permission from Ref. [25]. Copyright 2015, American Chemical Society. (c) Linear sweep voltammetry (LSV) results of different catalysts. (d) Potential-dependent Fes of the catalysts (shown on left). Reproduced with permission from Ref. [28]. Copyright 2018, Elsevier.

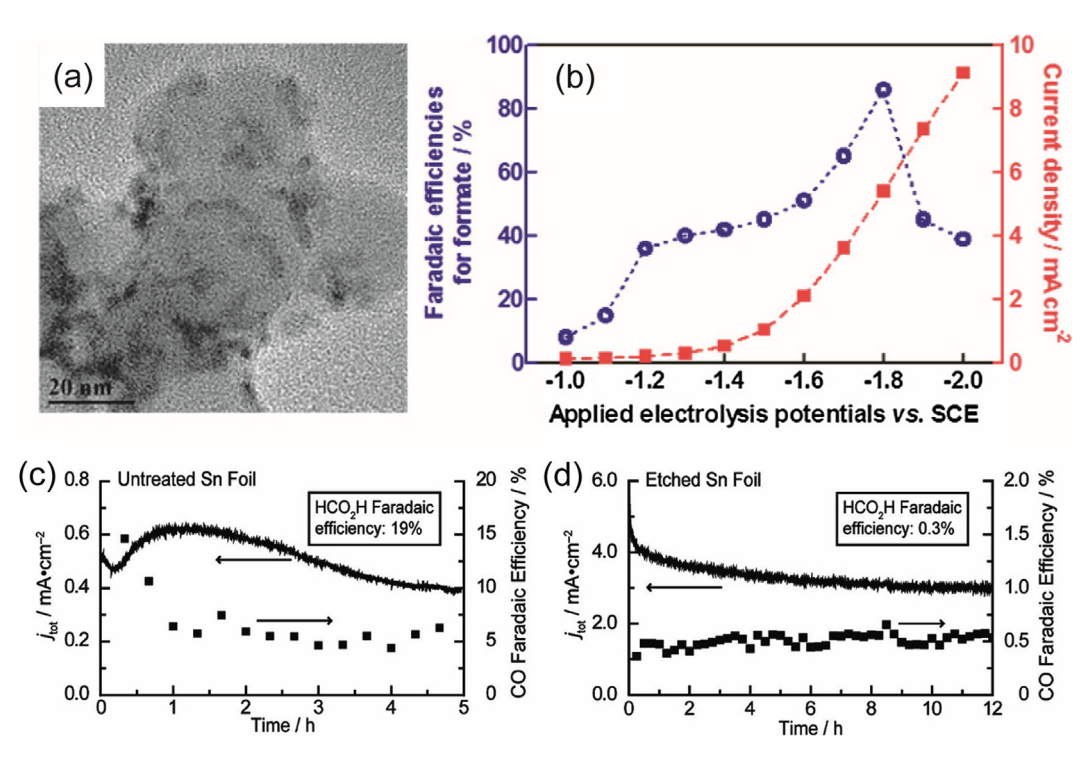


Fig. 4. (a) TEM image of \sim 5 nm tin oxide NPs on carbon black. (b) Potential-dependent FEs and current densities of reduced tin oxide NPs on ECR to formate. Reproduced with permission from Ref. [31]. Copyright 2014, American Chemical Society. (c) Time-dependent current density and CO FE for untreated Sn at -0.7 V (RHE). (d) Time-dependent current density and CO FE for etched Sn at -0.7 V (RHE). Reproduced with permission from Ref. [30]. Copyright 2012, American Chemical Society.

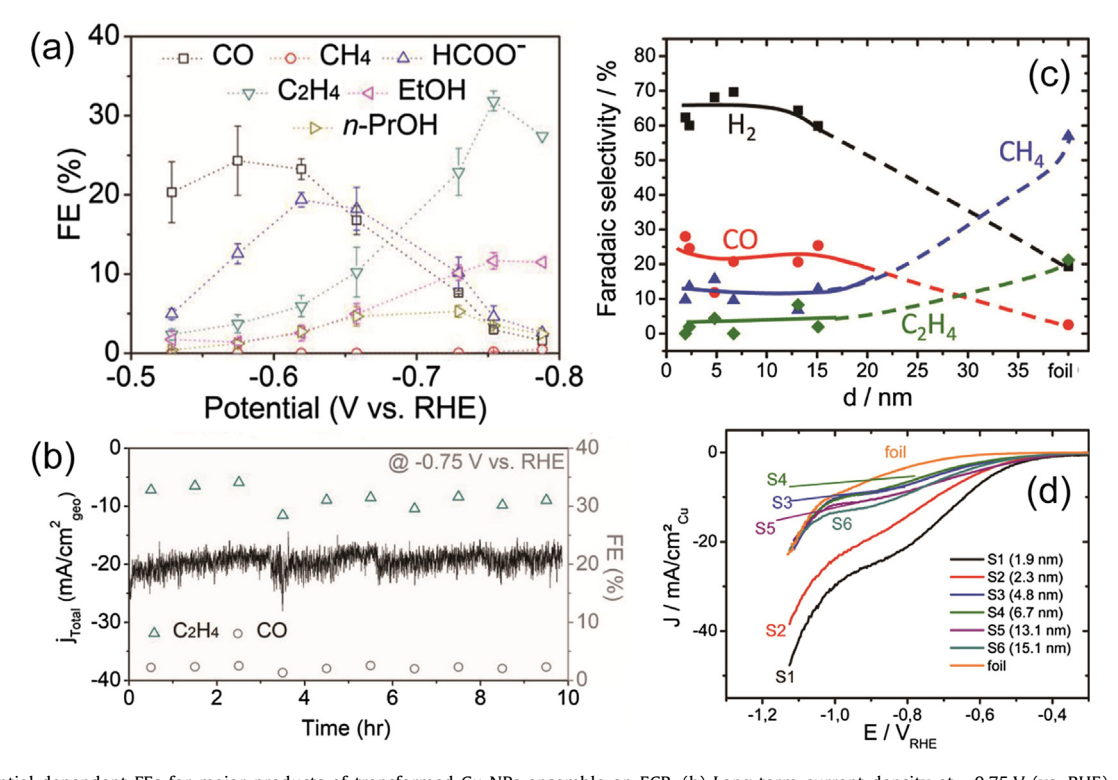


Fig. 5. (a) Potential-dependent FEs for major products of transformed Cu NPs ensemble on ECR. (b) Long-term current density at −0.75 V (vs. RHE). Reproduced with permission from Ref. [38]. Copyright 2017, National Academy of Sciences. (c) Faradic selectivity of products on Cu NPs. (d) LSV results on different sized Cu NPs. Reproduced with permission from Ref. [36]. Copyright 2014, American Chemical Society.

2.4. Copper catalysts

As noted above, Cu-based catalysts are special for the reduction of ${\rm CO_2}$ because they represent the only class of electrocatalysts that

can convert CO_2 to C_2 - C_3 hydrocarbons, whereas most other catalysts are only capable of producing C_1 products. For this reason, research on Cu-based ECR is especially important, and a large body of literatures has been published on this topic [33–37]. As one

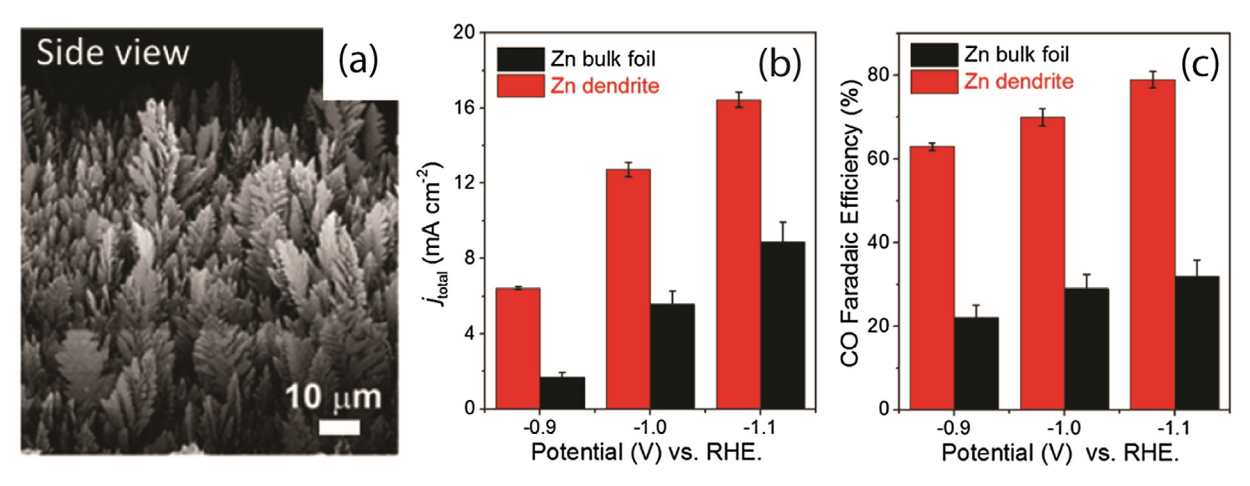


Fig. 6. (a) SEM image of Zn dendrites. (b) Potential-dependent current densities of bulk and dendritic Zn electrocatalysts. (c) Potential-dependent FE_{CO} of bulk and dendritic Zn electrocatalysts on ECR. Reproduced with permission from Ref. [39]. Copyright 2015, American Chemical Society.

example, Kim et al. investigated Cu NPs ensembles towards ECR to hydrocarbons. Among the Cu catalysts studied, optimal Cu NPs ensemble was shown to convert CO_2 to hydrocarbons with a 50% C_2 - C_3 FE at only -0.75 V (vs. RHE; Fig. 5) [38]. For another example, Reske et al. studied 2–15 nm sized Cu NPs for ECR. Catalytic activity and selectivity for H_2 and CO was increased, while hydrocarbon selectivity was suppressed with the deceasing Cu NPs size (Fig. 5) [36].

2.5. Other metal catalysts

In addition to the aforementioned examples, metal catalysts based on Zn [39,40], Pb [41], and Pd [42] have been studied. For instance, Rosen et al. reported electrodeposited Zn dendrites catalysts with enhanced catalytic performance for ECR over that of bulk Zn (Fig. 6). More specifically, the catalysts activity for Zn dendrites was an order of magnitude better, and a \sim 3 times FE $_{\rm CO}$ over bulk Zn was measured [39]. For another example, Zhang et al. reported a low-cost Zn electrode composed of multilayered Zn nanosheets (NSs). The Zn NSs showed a high FE $_{\rm CO}$ of \sim 86% at -1.13 V (vs. RHE), which is much higher than bulk Zn foil (Fig. 7). By density functional theory (DFT) calculations, the authors suggested that the high activity and selectivity of Zn NSs for the ECR is owing to their high density of edge sites [40].

3. Strategies for improving efficiency and selectivity

The factors important to the electrocatalytic activities of nanostructured catalysts include the sizes, exposed facets, compositions and morphologies of the catalysts. Below, we examine how these factors can be tuned for improved performance of ECR by these catalysts.

3.1. Size effects

With the development of nanosynthesis, metal NPs with different sizes can be readily produced. To the first order approximation, the size of NPs determines the ratio of atoms at different sites of a crystallite, including the corner, the edge and the surfaces. These different sites are expected to feature different coordination numbers and surface energies, which are critical factors to define the catalytic activities. Indeed, metal NPs of different sizes have been shown to exhibit different catalytic performance in ECR [20,22,25,43]. For example, Zhu et al. investigated the ECR performance on monodisperse 4, 6, 8, and 10 nm Au NPs. Among

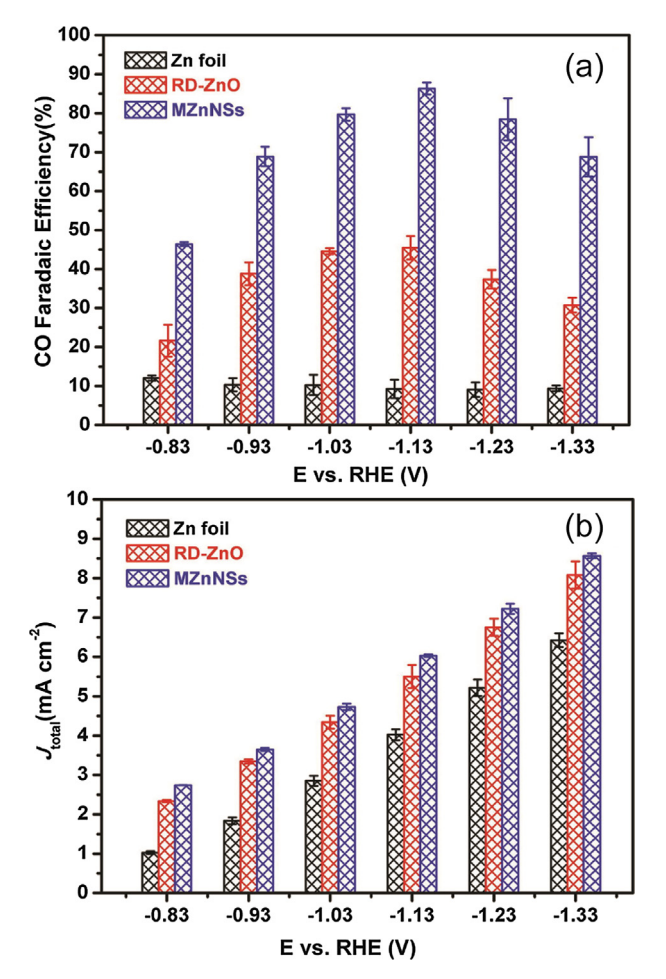


Fig. 7. Potential-dependent FE_{CO} (a) and current densities (b) of Zn foil, reduced disordered (RD) ZnO, and multilayered Zn NSs on ECR. Reproduced with permission from Ref. [40]. Copyright 2018, Elsevier.

them, 8 nm Au NPs exhibited the highest FE_{CO} of 90% at -0.67 V (vs. RHE; Fig. 8). By DFT calculations, the authors claimed that 8 nm Au NPs hold an optimum edge sites ratio for the highly selective CO formation, since the edge sites favor CO_2 reduction to CO while corner sites are active for HER [20].

Similarly, Gao et al. studied the ECR performance of Pd NPs with different sizes. The FE_{CO} and current density varied with the sizes.

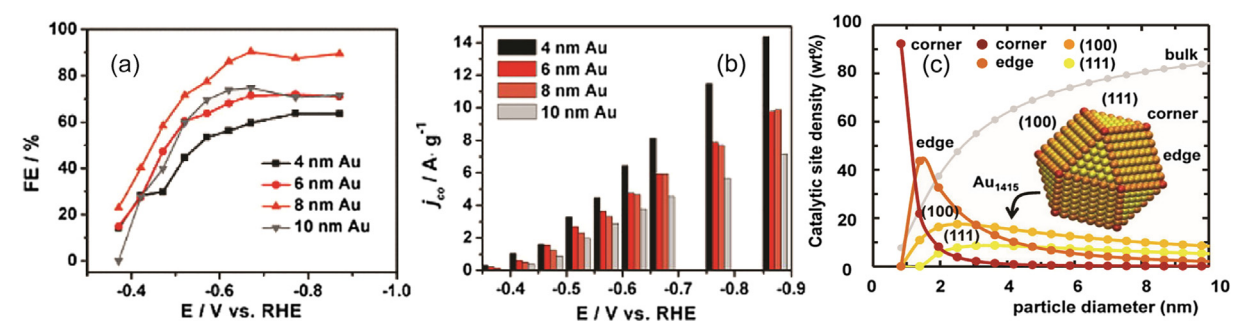


Fig. 8. (a) Potential-dependent FEs of Au NPs on carbon for ECR. (b) Potential-dependent current densities (mass activities) for CO formation of Au NPs on carbon. (c) Density of adsorption sites on closed-shell cuboctahedral Au clusters vs. the cluster diameter. Reproduced with permission from Ref. [20]. Copyright 2013, American Chemical Society.

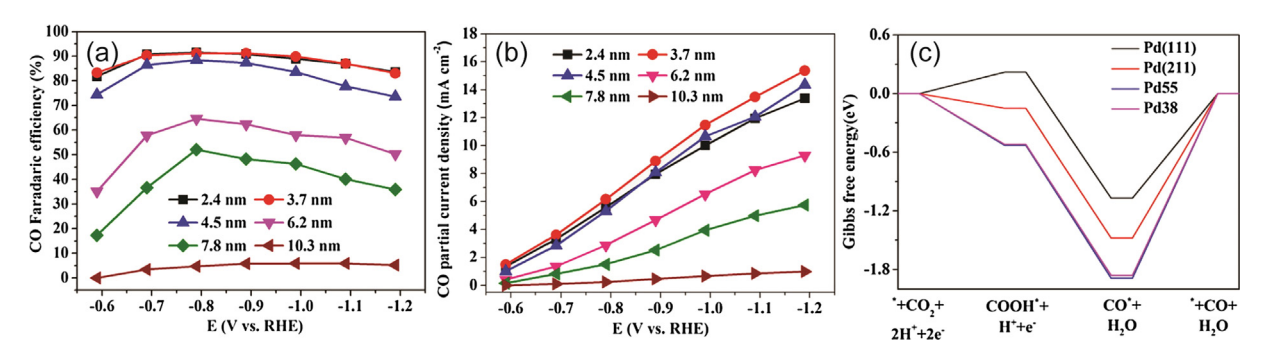


Fig. 9. Potential-dependent (a) FEs and (b) CO current densities of different sized Pd NPs on ECR. (c) Free energy diagram for CO₂ reduction to CO on Pd (1 1 1), Pd (2 1 1), Pd55, and Pd38. Reproduced with permission from Ref. [43]. Copyright 2015, American Chemical Society.

Based on their DFT calculations, the adsorption of CO₂ and formation of COOH* intermediate are easier on the edge and corner sites than on the terrace sites, whereas the competitive HER is comparable on all three sites (Fig. 9) [43]. The performance of Pd nanocatalysts can be tuned by varying their size due to the changing ratios of corner, edge and terrace sites.

3.2. Facet control

The correlation between the catalysts performance for ECR and the crystal orientation of the catalysts has been observed on different metals [26,34,44]. For instance, Lee et al. investigated concave rhombic dodecahedral Au nanocatalyst with various high-index facets for ECR (Fig. 10). Their results indicated that the concave rhombic dodecahedral Au nanocatalyst with high density of high-index facets possesses enhanced catalytic activity when compared with low-index Au NPs [44]. For another example, Klinkova et al. performed DFT simulations on Pd catalysts with different dominant facets for ECR. Their results indicate that there is a correlation between the catalytic performance and the coordination environment at the atomic level. They found that Pd nanocrystals with high-index facets are more resilient to CO poisoning and favor formic acid formation. Their experimental data supported the computational results (Fig. 10) [45]. The findings generated new insights into how to improve catalysts selectivity and activity by altering the facets of nanocatalysts.

3.3. Morphology effects

The correlation between the ECR performance and the morphology of catalysts has been discovered on different nanostructured metallic catalysts [24,46,47]. To this end, Hall et al. demonstrated that the diffusional limitations within the pores of the mesostructured electrode is the origin of hydrogen suppression in Au inverse

opal films (Fig. 11). The optimal mesostructured electrode generates a 75% FE for CO production at $-0.40\,\mathrm{V}$ (vs. RHE) [47]. Ma et al. investigated the effect of Cu NW morphology on the performance of ECR in aqueous solutions. By altering the length and density of Cu NWs, they were able to control hydrocarbon formation on Cu NWs arrays at a fixed potential (Fig. 11). They ascribed the effect to how the local pH was dependent on the Cu NW morphology. They further proposed that enhanced C_2 products formation on increased Cu NWs length was due to enhanced CO dimerization at higher local pH [46].

3.4. Surface modifications

A peculiar treatment that first oxidizes and then reduces metals (such as Au [19], Ag [48] and Cu [33]) has been shown to improve the performance of metallic electrodes in ECR dramatically. This method is thought to change the surface atomic arrangements and, thus, create more active sites to enhance the ECR performance. For example, Chen et al. demonstrated that oxide-derived Au NPs by reduction of Au oxide film exhibited high selectivity of ECR to CO with low overpotentials and long catalyst lifetimes over polycrystalline Au (Fig. 12). They suggested that the enhanced catalytic performance was due to increased stabilization of CO_2^- intermediate on the surface of oxide-derived Au, which was supported by electrokinetic studies [19]. Similarly, Ma et al. presented that the nanostructured Ag resulting from Ag oxide was able to electrochemically reduce CO_2 to CO with \sim 80% FE at a moderate overpotential of 0.49 V (Fig. 12) [48].

3.5. Composition control

Another class of metallic nanocatalysts that have been studied widely for ECR was nanoparticles with multiple elements [49–52]. For instance, Ma et al. investigated a series of bimetallic

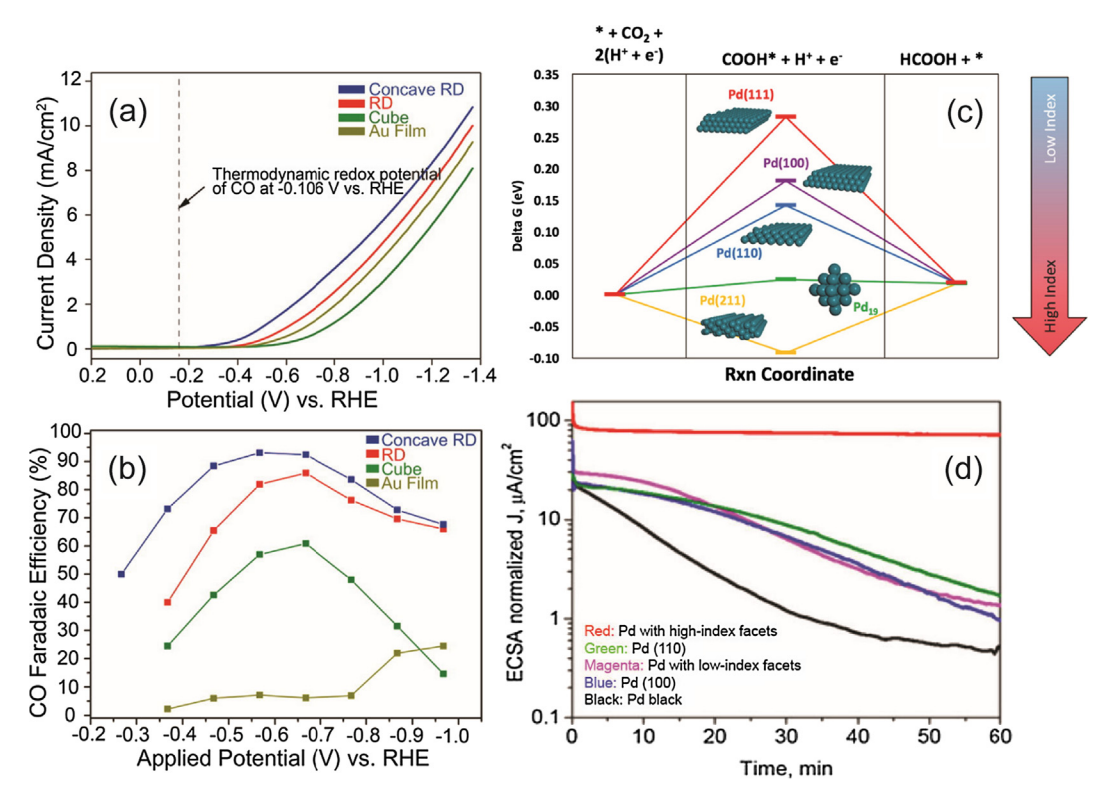


Fig. 10. (a) LSV results of different Au catalysts. (b) Potential-dependent CO FE of different Au catalysts. Reproduced with permission from Ref. [44]. Copyright 2015, American Chemical Society. (c) Free energy diagrams for ECR to formic acid on Pd(1 1 1), Pd(1 0 0), Pd(1 1 0), Pd(2 1 1), and Pd₁₉ cluster. (d) Electrochemical surface area (ECSA) normalized current densities of different Pd catalysts at -0.2 V (vs. RHE). Reproduced with permission from Ref. [45]. Copyright 2016, American Chemical Society.

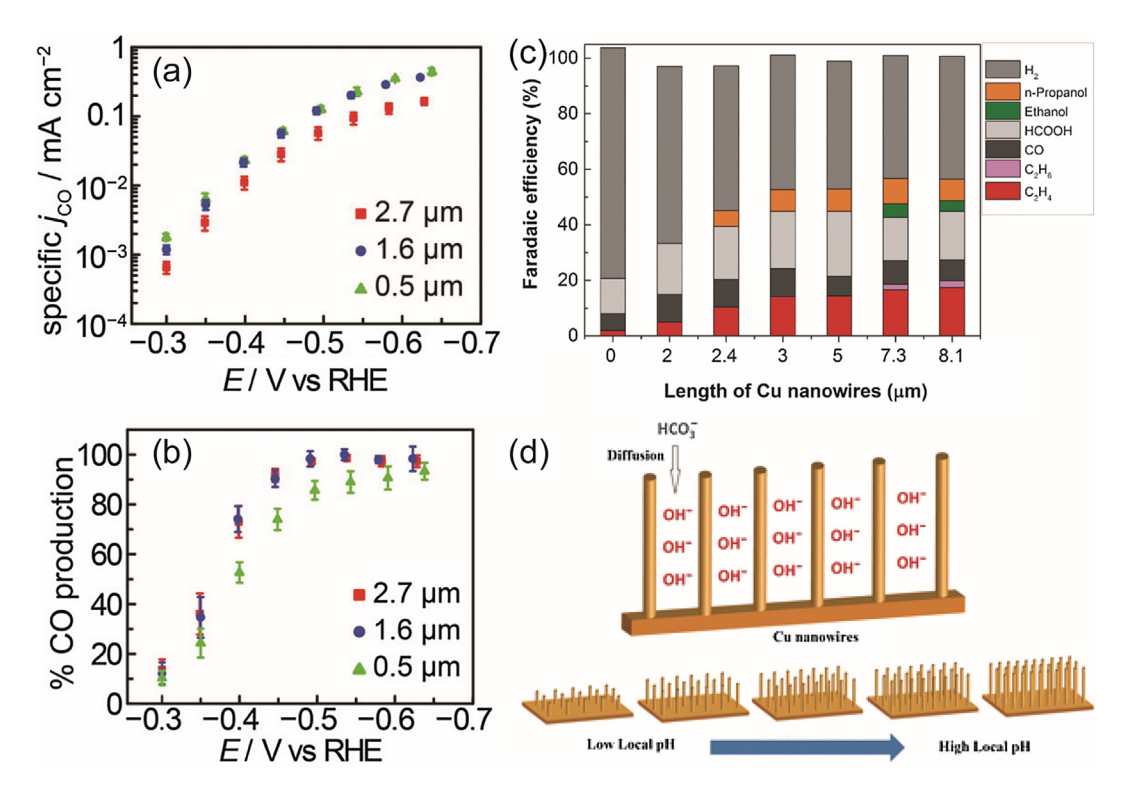


Fig. 11. (a) Potential-dependent specific activity for CO evolution on different thickness Au catalysts. (b) Potential-dependent CO FE on different thickness Au catalysts. Reproduced with permission from Ref. [47]. Copyright 2015, American Chemical Society. (c) FEs of H₂, n-propanol, ethanol, HCOOH, CO, C₂H₆ and C₂H₄ on Cu NWs arrays with different length at -1.1 V (vs. RHE). (d) Schematic illustration of the diffusion of electrolytes into Cu NWs arrays. Reproduced with permission from Ref. [46]. Copyright 2016, Wiley-VCH.

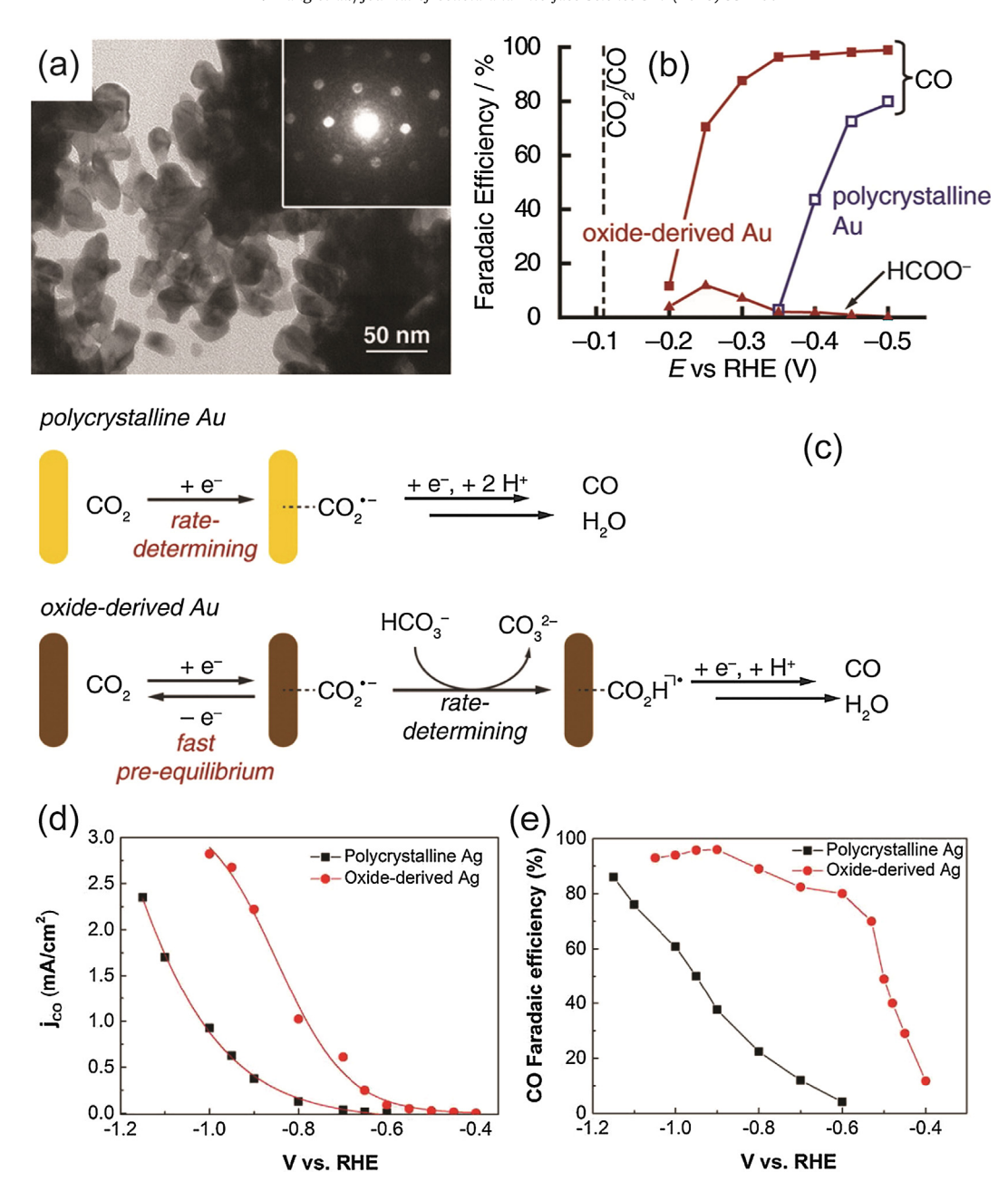


Fig. 12. (a) TEM image of oxide-derived Au NPs. Inset: corresponding nanobeam electro diffraction pattern. (b) Potential-dependent FEs of CO and HCOO- on oxide-derived Au and polycrystalline Au electrodes. (c) Proposed Mechanisms for ECR to CO on Polycrystalline Au and Oxide-Derived Au. Reproduced with permission from Ref. [19]. Copyright 2012, American Chemical Society. (d) Potential-dependent CO current densities of polycrystalline Ag and oxide-derived Ag. (e) Potential-dependent CO FE of polycrystalline Ag and oxide-derived Ag. Reproduced with permission from Ref. [48]. Copyright 2016, Wiley-VCH.

Cu-Pd catalysts with different elemental ratios and atomic arrangements. They pointed out that the selectivity in ECR products could be tuned by varying the composition of bimetallic Cu-Pd catalysts. The tunability of the catalysts selectivity was attributed to the geometric effects based on their subsequent studies (Fig. 13) [53]. In another example, Kim et al. found that the selectivity in ECR products could be controlled by tuning the composition of Au-Cu bimetallic NPs, as dictated by the electronic effect and the geometric effect (Fig. 13) [52].

4. Summary and perspectives

Due to the severity of the problems caused by the rapid increase of CO₂ concentrations in our atmosphere, research on ECR is one of

the most vibrant in recent years. It has attracted researchers with different backgrounds, ranging from chemistry and materials science to physics and engineering. Great progress has been made; significant challenges remain. Our goal of compiling this *Article* is provide a focused discussion on nanostructured metallic catalysts for ECR in aqueous solutions. Within this context, various types of metallic nanocatalysts based on their different selectivity for products are reviewed. Several important factors including sizes, exposed facets, compositions and morphologies of the catalysts that can be tuned to improve activity and selectivity of nanocatalysts for ECR are discussed.

A representative trend of research on ECR has been on how to prepare nanostructured catalysts with high activity and selectivity. In the meanwhile, significant efforts have been devoted to gaining a deeper understanding of the mechanisms, especially at the

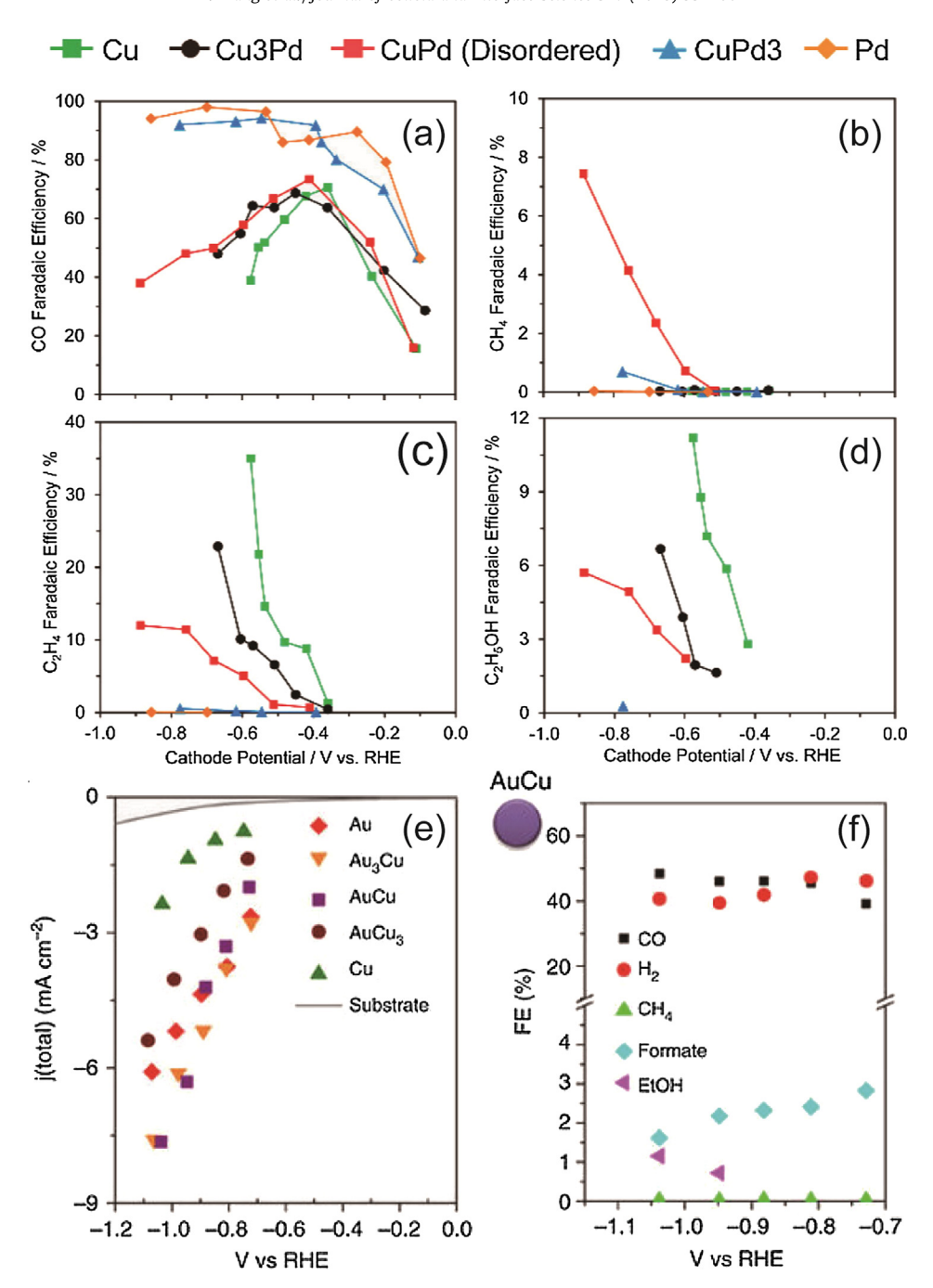


Fig. 13. Potential-dependent FEs for (a) CO, (b) CH₄, (c) C₂H₄, and (d) C₂H₅OH of catalysts with different Cu:Pd ratios on ECR. Reproduced with permission from Ref. [53]. Copyright 2017, American Chemical Society. (e) Potential-dependent current densities of Au-Cu bimetallic NPs. (f) Potential-dependent FEs for each product of AuCu catalysts. Reproduced with permission from Ref. [52]. Copyright 2014, Springer Nature.

molecular level. To this end, the development of computational chemistry has played a tremendous role. It has made studies of the reaction mechanisms at the atomic and molecular level accessible by methods such as DFT calculations. Moving forward, it will be of critical importance to verify the various hypotheses supported by computational calculations using advanced characterization tools, particularly in situ and in operando ones. Information of the catalysts and the reactions intermediates under normal conditions will be critically important to advancing our knowledge.

Most of the efforts in finding better catalysts and understanding the reaction mechanisms are guided to enable practical CO₂ reduction applications. For this purpose, we must bear in mind several important criteria. For instance, the catalysts are expected to feature high activity as measured by small overpotentials, which is necessary for high energy efficiency. In the meanwhile, high selectivity is of paramount importance. That is, we desire high faradic efficiency for desired products. This is especially true for the synthesis of high-value chemicals. For large scale implementations, the catalysts will likely be composed of earth-abundant elements. Lastly, we note that the durability of the catalyst is also highly important. Given that most large scale electrochemical implementations are carried out in either highly acidic or basic electrolytes to minimize polarization in the electrolyte, it is critical to consider how to maintain the stability of the catalyst. The last point could

prove particularly challenging for nanoscale catalysts as surface reconstruction and reorganization at such a length scale is well known. Despite these challenges, we are at an exciting time in doing research in this area thanks to the concerted efforts by a large research community.

Acknowledgements

The authors are grateful for financial support by a Startup Grant (39837130) from Nanjing Tech University and a SICAM Fellowship by Jiangsu National Synergetic Innovation Center for Advanced Materials. Y.W. thanks China Postdoctoral Administration and Nanjing Tech University for a postdoctoral fellowship. D.W. thanks financial support from the NSF (CBET 1703663 and CBET 1703655), the Department of Energy (DE-EE0008086), and the Massachusetts Clean Energy Center.

Conflict of interest

The authors declare no conflict of interest.

References

- [1] W.-H. Wang, Y. Himeda, J.T. Muckerman, G.F. Manbeck, E. Fujita, CO₂ hydrogenation to formate and methanol as an alternative to photo- and electrochemical CO₂ reduction, Chem. Rev. 115 (2015) 12936–12973.
- [2] J.-P. Jones, G.K.S. Prakash, G.A. Olah, Electrochemical CO₂ reduction: recent advances and current trends, Isr. J. Chem. 54 (2014) 1451–1466.
- [3] J. Durst, A. Rudnev, A. Dutta, Y. Fu, J. Herranz, V. Kaliginedi, A. Kuzume, A.A. Permyakova, Y. Paratcha, P. Broekmann, T.J. Schmidt, Electrochemical CO₂ reduction a critical view on fundamentals, materials and applications, Chimia (Aarau) 69 (2015) 769–776.
- [4] E.E. Benson, C.P. Kubiak, A.J. Sathrum, J.M. Smieja, Electrocatalytic and homogeneous approaches to conversion of CO₂ to liquid fuels, Chem. Soc. Rev. 38 (2009) 89–99.
- [5] M. Rakowski Dubois, D.L. Dubois, Development of molecular electrocatalysts for CO₂ reduction and H₂ production/oxidation, Acc. Chem. Res. 42 (2009) 1974–1982.
- [6] J. Schneider, H. Jia, J.T. Muckerman, E. Fujita, Thermodynamics and kinetics of CO₂, CO, and H⁺ binding to the metal centre of CO₂ reduction catalysts, Chem. Soc. Rev. 41 (2012) 2036–2051.
- [7] Y. Wang, J. Liu, Y. Wang, A.M. Al-Enizi, G. Zheng, Tuning of CO₂ reduction selectivity on metal electrocatalysts, Small 1701809 (2017).
- [8] Q. Lu, F. Jiao, Electrochemical CO₂ reduction: electrocatalyst, reaction mechanism, and process engineering, Nano Energy 29 (2016) 439–456.
- [9] R. Kortlever, J. Shen, K.J.P. Schouten, F. Calle-Vallejo, M.T.M. Koper, Catalysts and reaction pathways for the electrochemical reduction of carbon dioxide, J. Phys. Chem. Lett. 6 (2015) 4073–4082.
- [10] Q. Lu, J. Rosen, F. Jiao, Nanostructured metallic electrocatalysts for carbon dioxide reduction, ChemCatChem 7 (2015) 38–47.
- [11] Y. Hori, Electrochemical CO2 Reduction on Metal Electrodes, in: Modern Aspects of Electrochemistry, Springer, New York, 2008, pp. 89–189.
- [12] B. Khezri, A.C. Fisher, M. Pumera, CO₂ reduction: the quest for electrocatalytic materials, J. Mater. Chem. A 5 (2017) 8230–8246.
- [13] D.D. Zhu, J.L. Liu, S.Z. Qiao, Recent advances in inorganic heterogeneous electrocatalysts for reduction of carbon dioxide, Adv. Mater. 28 (2016) 3423– 3452.
- [14] L. Zhang, Z.-J. Zhao, J. Gong, Nanostructured materials for heterogeneous electrocatalytic CO₂ reduction and their related reaction mechanisms, Angew. Chem. Int. Ed. 56 (2017) 11326–11353.
- [15] D.R. Kauffman, J. Thakkar, R. Siva, C. Matranga, P.R. Ohodnicki, C. Zeng, R. Jin, Efficient electrochemical CO₂ conversion powered by renewable energy, ACS Appl. Mat. Interfaces 7 (2015) 15626–15632.
- [16] J. Liu, C. Guo, A. Vasileff, S. Qiao, Nanostructured 2D materials: prospective catalysts for electrochemical CO₂ reduction, Small Methods 1 (2017) 1600006.
- [17] A. Wuttig, Y. Surendranath, Impurity ion complexation enhances carbon dioxide reduction catalysis, ACS Catal. 5 (2015) 4479–4484.
- [18] D.R. Kauffman, D. Alfonso, C. Matranga, H. Qian, R. Jin, Experimental and computational investigation of Au₂₅ clusters and CO₂: a unique interaction and enhanced electrocatalytic activity, J. Am. Chem. Soc. 134 (2012) 10237–10243.
- [19] Y. Chen, C.W. Li, M.W. Kanan, Aqueous CO₂ reduction at very low overpotential on oxide-derived Au nanoparticles, J. Am. Chem. Soc. 134 (2012) 19969– 19972.
- [20] W. Zhu, R. Michalsky, Ö. Metin, H. Lv, S. Guo, C.J. Wright, X. Sun, A.A. Peterson, S. Sun, Monodisperse Au nanoparticles for selective electrocatalytic reduction of CO₂ to CO, J. Am. Chem. Soc. 135 (2013) 16833–16836.

- [21] J.A. Trindell, J. Clausmeyer, R.M. Crooks, Size stability and H₂/CO selectivity for Au nanoparticles during electrocatalytic CO₂ reduction, J. Am. Chem. Soc. 139 (2017) 16161–16167.
- [22] H. Mistry, R. Reske, Z. Zeng, Z.-J. Zhao, J. Greeley, P. Strasser, B.R. Cuenya, Exceptional size-dependent activity enhancement in the electroreduction of CO₂ over Au nanoparticles, J. Am. Chem. Soc. 136 (2014) 16473–16476.
- [23] X. Feng, K. Jiang, S. Fan, M.W. Kanan, Grain-boundary-dependent CO₂ electroreduction activity, J. Am. Chem. Soc. 137 (2015) 4606–4609.
- [24] W. Zhu, Y.-J. Zhang, H. Zhang, H. Lv, Q. Li, R. Michalsky, A.A. Peterson, S. Sun, Active and selective conversion of CO₂ to CO on ultrathin Au nanowires, J. Am. Chem. Soc. 136 (2014) 16132–16135.
- [25] C. Kim, H.S. Jeon, T. Eom, M.S. Jee, H. Kim, C.M. Friend, B.K. Min, Y.J. Hwang, Achieving selective and efficient electrocatalytic activity for CO₂ reduction using immobilized silver nanoparticles, J. Am. Chem. Soc. 137 (2015) 13844– 13850.
- [26] X. Peng, S.G. Karakalos, W.E. Mustain, Preferentially oriented Ag nanocrystals with extremely high activity and Faradaic efficiency for CO₂ electrochemical reduction to CO, ACS Appl. Mat. Interfaces 10 (2018) 1734–1742.
- [27] Y.-C. Hsieh, S.D. Senanayake, Y. Zhang, W. Xu, D.E. Polyansky, Effect of chloride anions on the synthesis and enhanced catalytic activity of silver nanocoral electrodes for CO₂ electroreduction, ACS Catal. 5 (2015) 5349–5356.
- [28] S. Liu, X.-Z. Wang, H. Tao, T. Li, Q. Liu, Z. Xu, X.-Z. Fu, J.-L. Luo, Ultrathin 5-fold twinned sub-25 nm silver nanowires enable highly selective electroreduction of CO₂ to CO, Nano Energy 45 (2018) 456–462.
- [29] S. Liu, H. Tao, L. Zeng, Q. Liu, Z. Xu, Q. Liu, J.-L. Luo, Shape-dependent electrocatalytic reduction of CO₂ to CO on triangular silver nanoplates, J. Am. Chem. Soc. 139 (2017) 2160–2163.
- [30] Y. Chen, M.W. Kanan, Tin oxide dependence of the CO₂ reduction efficiency on tin electrodes and enhanced activity for tin/tin oxide thin-film catalysts, J. Am. Chem. Soc. 134 (2012) 1986–1989.
- [31] S. Zhang, P. Kang, T.J. Meyer, Nanostructured tin catalysts for selective electrochemical reduction of carbon dioxide to formate, J. Am. Chem. Soc. 136 (2014) 1734–1737.
- [32] J. Medina-Ramos, R.C. Pupillo, T.P. Keane, J.L. DiMeglio, J. Rosenthal, Efficient conversion of CO₂ to CO using tin and other inexpensive and easily prepared post-transition metal catalysts, J. Am. Chem. Soc. 137 (2015) 5021–5027.
- [33] C.W. Li, M.W. Kanan, CO₂ reduction at low overpotential on Cu electrodes resulting from the reduction of thick Cu₂O films, J. Am. Chem. Soc. 134 (2012) 7231–7234.
- [34] Y. Li, F. Cui, M.B. Ross, D. Kim, Y. Sun, P. Yang, Structure-sensitive CO₂ electroreduction to hydrocarbons on ultrathin 5-fold twinned copper nanowires, Nano Lett. 17 (2017) 1312–1317.
- [35] S. Sen, D. Liu, G.T.R. Palmore, Electrochemical reduction of CO₂ at copper nanofoams, ACS Catal. 4 (2014) 3091–3095.
- [36] R. Reske, H. Mistry, F. Behafarid, B. Roldan Cuenya, P. Strasser, Particle size effects in the catalytic electroreduction of CO₂ on Cu nanoparticles, J. Am. Chem. Soc. 136 (2014) 6978–6986.
- [37] O.A. Baturina, Q. Lu, M.A. Padilla, L. Xin, W. Li, A. Serov, K. Artyushkova, P. Atanassov, F. Xu, A. Epshteyn, T. Brintlinger, M. Schuette, G.E. Collins, CO₂ electroreduction to hydrocarbons on carbon-supported Cu nanoparticles, ACS Catal. 4 (2014) 3682–3695.
- [38] D. Kim, C.S. Kley, Y. Li, P. Yang, Copper nanoparticle ensembles for selective electroreduction of CO₂ to C₂-C₃ products, PNAS 114 (2017) 10560–10565.
 [39] J. Rosen, G.S. Hutchings, Q. Lu, R.V. Forest, A. Moore, F. Jiao, Electrodeposited Zn
- [39] J. Rosen, G.S. Hutchings, Q. Lu, R.V. Forest, A. Moore, F. Jiao, Electrodeposited Zn dendrites with enhanced CO selectivity for electrocatalytic CO₂ reduction, ACS Catal, 5 (2015) 4586–4591.
- [40] T. Zhang, X. Li, Y. Qiu, P. Su, W. Xu, H. Zhong, H. Zhang, Multilayered Zn nanosheets as an electrocatalyst for efficient electrochemical reduction of CO₂, I. Catal. 357 (2018) 154–162.
- [41] C.H. Lee, M.W. Kanan, Controlling H^* vs CO_2 reduction selectivity on Pb electrodes, ACS Catal. 5 (2015) 465–469.
- [42] X. Min, M.W. Kanan, Pd-catalyzed electrohydrogenation of carbon dioxide to formate: high mass activity at low overpotential and identification of the deactivation pathway, J. Am. Chem. Soc. 137 (2015) 4701–4708.
 [43] D. Gao, H. Zhou, J. Wang, S. Miao, F. Yang, G. Wang, J. Wang, X. Bao, Size-
- [43] D. Gao, H. Zhou, J. Wang, S. Miao, F. Yang, G. Wang, J. Wang, X. Bao, Size-dependent electrocatalytic reduction of CO₂ over Pd nanoparticles, J. Am. Chem. Soc. 137 (2015) 4288–4291.
- [44] H.-E. Lee, K.D. Yang, S.M. Yoon, H.-Y. Ahn, Y.Y. Lee, H. Chang, D.H. Jeong, Y.-S. Lee, M.Y. Kim, K.T. Nam, Concave rhombic dodecahedral Au nanocatalyst with multiple high-index facets for CO₂ reduction, ACS Nano 9 (2015) 8384–8393.
- [45] A. Klinkova, P. De Luna, C.-T. Dinh, O. Voznyy, E.M. Larin, E. Kumacheva, E.H. Sargent, Rational design of efficient palladium catalysts for electroreduction of carbon dioxide to formate, ACS Catal. 6 (2016) 8115–8120.
- [46] M. Ma, K. Djanashvili, W.A. Smith, Controllable hydrocarbon formation from the electrochemical reduction of CO₂ over Cu nanowire arrays, Angew. Chem. Int. Ed. 55 (2016) 6680–6684.
- [47] A.S. Hall, Y. Yoon, A. Wuttig, Y. Surendranath, Mesostructure-induced selectivity in CO₂ reduction catalysis, J. Am. Chem. Soc. 137 (2015) 14834– 14837.
- [48] M. Ma, B.J. Trześniewski, J. Xie, W.A. Smith, Selective and efficient reduction of carbon dioxide to carbon monoxide on oxide-derived nanostructured silver electrocatalysts, Angew. Chem. Int. Ed. 55 (2016) 9748–9752.
- [49] Z. Xu, E. Lai, Y. Shao-Horn, K. Hamad-Schifferli, Compositional dependence of the stability of AuCu alloy nanoparticles, Chem. Commun. 48 (2012) 5626– 5628

- [50] S. Back, J.-H. Kim, Y.-T. Kim, Y. Jung, Bifunctional interface of Au and Cu for improved ${\rm CO_2}$ electroreduction, ACS Appl. Mat. Interfaces 8 (2016) 23022–23027.
- [51] C. Shan, E.T. Martin, D.G. Peters, J.M. Zaleski, Site-selective growth of AgPd nanodendrite-modified Au nanoprisms: high electrocatalytic performance for CO₂ reduction, Chem. Mater. 29 (2017) 6030–6043.
- [52] D. Kim, J. Resasco, Y. Yu, A.M. Asiri, P. Yang, Synergistic geometric and electronic effects for electrochemical reduction of carbon dioxide using gold-copper bimetallic nanoparticles, Nat. Commun. 5 (2014) 4948.
 [53] S. Ma, M. Sadakiyo, M. Heima, R. Luo, R.T. Haasch, J.I. Gold, M. Yamauchi, P.J.A.
- [53] S. Ma, M. Sadakiyo, M. Heima, R. Luo, R.T. Haasch, J.I. Gold, M. Yamauchi, P.J.A. Kenis, Electroreduction of carbon dioxide to hydrocarbons using bimetallic Cu– Pd catalysts with different mixing patterns, J. Am. Chem. Soc. 139 (2017) 47–50.